

# Prospective Evaluation of Semiquantitative Strain Ratio and Quantitative 2D Ultrasound Shear Wave Elastography (SWE) in Association with TIRADS Classification for Thyroid Nodule Characterization

## Prospektive Evaluierung der semiquantitativen Kompressionselastografie und der quantitativen 2D-Scherwellenultraschall-elastografie (SWE) in Verbindung mit der TIRADS-Klassifikation zur Charakterisierung von Schilddrüsenknoten

### Authors

Vito Cantisani<sup>1</sup>, Emanuele David<sup>2</sup>, Hektor Grazhdani<sup>3</sup>, Antonello Rubini<sup>1</sup>, Maija Radzina<sup>4</sup>, Christoph F. Dietrich<sup>5</sup>, Cosimo Durante<sup>6</sup>, Livia Lamartina<sup>6</sup>, Giorgio Grani<sup>6</sup>, Ascoli Valeria<sup>7</sup>, Daniela Bosco<sup>7</sup>, Cira Di Gioia<sup>7</sup>, Fabrizio Maria Frattaroli<sup>8</sup>, Vito D'Andrea<sup>8</sup>, Corrado De Vito<sup>9</sup>, Daniele Fresilli<sup>10</sup>, Ferdinando D'Ambrosio<sup>1</sup>, Laura Giacomelli<sup>8</sup>, Carlo Catalano<sup>1</sup>

### Affiliations

- 1 Department of Radiology, Sapienza-University of Rome, Rome, Italy
- 2 Radiology Unit, Papardo-Hospital, Messina, Italy
- 3 Poliambulatorio Roma Eur, Associazione dei Cavalieri Italiani Sovrano Militare Ordine di Malta, Rome, Italy
- 4 Diagnostic Radiology Institute, P. Stradina Clinical University-Hospital, Riga, Latvia
- 5 Innere Medizin 2, Caritas-Krankenhaus, Bad Mergentheim, Germany
- 6 Department of Internal Medicine and Medical Specialities, Sapienza-University of Rome, Rome, Italy
- 7 Department of Pathological Anatomy and Cytodiagnostic, Sapienza-University of Rome, Rome, Italy
- 8 Department of Surgical Sciences, Sapienza-University of Rome, Rome, Italy
- 9 Department of Public Health and Infectious Diseases, Sapienza-University of Rome, Rome, Italy
- 10 University Sapienza, Department of Radiological Sciences, Rome, Italy

### Key words

thyroid nodule characterization, TIRADS, elastography

received 02.12.2017

accepted 24.01.2019

### Bibliography

DOI <https://doi.org/10.1055/a-0853-1821>

Published online: May 28, 2019

Ultraschall in Med 2019; 40: 495–503

© Georg Thieme Verlag KG, Stuttgart · New York

ISSN 0172-4614

### Correspondence

Dr. Vito Cantisani

Department of Radiology, Sapienza-University of Rome,

Viale Regina Elena, 324, 00161 Rome, Italy

Tel.: ++ 39/34 71 74 39 47

Fax: ++ 39/0 64 45 56 02

[vito.cantisani@uniroma1.it](mailto:vito.cantisani@uniroma1.it)

### ABSTRACT

**Purpose** To evaluate the diagnostic performance of strain ratio elastography (SRE) and shear wave elastography (SWE) alone and in combination with Thyroid Imaging Reporting and Data System (TIRADS) classification parameters to improve differentiation between benign and malignant thyroid nodules.

**Materials and Methods** In this prospective study benign (n = 191) and malignant (n = 52) thyroid nodules were examined with high-resolution ultrasound (US) features using the TIRADS lexicon and SRE semiquantitative and SWE quantitative findings using histology or cytology as the gold standard with a 12-month follow-up. Sensitivity (Se), specificity (Sp) and the area under the ROC curve (AUROC) were used to evaluate the diagnostic performance of each feature and combinations of the methods.

**Results** TIRADS score showed a sensitivity of 59.6%, a specificity of 83.8% with an AUROC of 0.717, a PPV of 50.0% and an NPV of 88.4%. SRE yielded the highest performance with a

sensitivity of 82.7%, a specificity of 92.7% with AUROC of 0.877, a PPV 75.4% and an NPV of 95.2%. SWE (kPa) had a sensitivity and specificity of 67.3% and 82.7%, respectively, with an AUROC of 0.750, a PPV of 51.5% and an NPV of 90.3%. Differences were significant for SRE only but not for SWE.

**Conclusion** Ultrasound elastography may improve thyroid nodule discrimination. In particular, SRE has a better performance than TIRADS classification, while their combination improves sensitivity.

## ZUSAMMENFASSUNG

**Ziel der Studie** Die Studie erfolgte, um die diagnostische Genauigkeit der Kompressionselastografie (SRE) und Scherwellenelastografie (SWE) einzeln und in Kombination mit der Thyroid-Imaging-Reporting-and-Data-System (TIRADS)-Klassifikation zu untersuchen, um eine verbesserte Differenzierung von benignen und malignen Schilddrüsenknoten zu ermöglichen.

**Patienten und Methoden** In dieser prospektiven Studie wurden gutartige (n = 191) und bösartige (n = 52) Schilddrü-

senknoten mittels Ultraschall, SRE und SWE untersucht und die Daten mit der TIRADS-Klassifikation verglichen. Gutartige Läsionen wurden 12 Monate nachbeobachtet. Sensitivität (Se), Spezifität (Sp) und der Bereich unter der ROC-Kurve (Area-under-the-ROC-Curve – AUROC) sowie der positive prädiktive (PPV) und der negative prädiktive Wert (NPV) wurden berechnet, um die diagnostische Genauigkeit der einzelnen und kombinierten Methoden zu vergleichen.

**Ergebnisse** Der TIRADS-Score zeigte eine Se von 59,6% und eine Sp von 83,8% mit einer AUROC von 0,717. Der PPV lag bei 50,0% und der NPV bei 88,4%. SRE (in Klammern SWE (kPa)) erreichte die höchste Genauigkeit mit einer Se von 82,7% (67,3%) und einer Sp von 92,7% (82,7%); die AUROC lag bei 0,877 (0,750). Die Unterschiede zwischen SRE und SWE waren statistisch signifikant ( $p < 0,05$ ).

**Schlussfolgerung** Die Ultraschallelastografie kann eine verbesserte Differenzierung von Schilddrüsenknoten ermöglichen. Insbesondere zeigt SRE bessere Ergebnisse als TIRADS, während die kombinierte Anwendung die Sensitivität verbessert.

## Introduction

High-resolution ultrasound (US) has been established as the first imaging modality for the characterization of thyroid nodules. Given the high prevalence (19–68%) and incidence of thyroid nodules in the general population and the high rate of non-malignant lesions (>85–95%), the role of US has expanded [1]. Several guidelines indicate how to stratify the ‘risk-of-malignancy’ with US and to follow appropriate diagnostic algorithms [1–3], and several Thyroid Imaging Reporting and Data Systems (TIRADS) [1–6] have recently been proposed as a tool for uniform reporting and consistent evaluation. This risk stratification should guide the indication for fine needle aspiration biopsy (FNAB) that is generally required for nodules >10 mm with suspicious US signs or those with indeterminate signs >15 mm, aiming to reduce the overall number of biopsies [7]. Cytology itself has a reported specificity of 60–98% and a highly variable sensitivity (54–90%) [8, 9] with too many non-diagnostic reports [10–13].

Ultrasound elastography (USE) has been proposed as a promising additional tool. USE evaluates the increase of stiffness in a thyroid nodule as a sign of malignancy [14–18]. The use of USE methods has been incorporated into international guidelines published by WFUMB (World Federation for Ultrasound in Medicine and Biology) [19] and EFSUMB (European Federation of Societies for Ultrasound in Medicine and Biology) [20], that also provide technical details, advantages and limitations for strain elastography (SRE) and quantitative 2D ultrasound shear wave elastography (SWE).

To the best of our knowledge, no original paper assessing the contributions of Kwak TIRADS and elastography modalities has been published. In the present study the diagnostic performance

of SRE and SWE in comparison and in association with the Kwak-TIRADS was prospectively evaluated for thyroid nodule differentiation.

## Materials and methods

### Enrollment

The local review board approved the protocol, and all patients gave written informed consent. From January 2014 to March 2016, patients with thyroid nodules who had not undergone previous radiation therapy were included. Exclusion criteria were: nodules not suitable for USE assessment [13] due to cystic component >50% of the nodule; egg-shell calcifications; nodules occupying >80% of the lobe; patients without a cytology or histology result.

### TIRADS lexicon

All nodules were evaluated through TIRADS lexicon, assessing the internal component, echogenicity, margins, presence of calcifications, and shape [6], SRE and SWE (kPa). US was performed using a premium ultrasound unit with a 5–14 MHz linear array transducer (Aplio 500 Platinum, Canon Medical Systems, Nasu, Japan). Every nodule was measured and described evaluating composition (solid, mixed, or cystic), echogenicity (hyper-, iso-, hypoechoic, or markedly hypoechoic), margins (regular, microlobulated; irregular/spiculated), calcifications (absent, micro- or macrocalcifications), shape (taller-than-wide shape is recorded when the anteroposterior diameter is greater than the transverse one; wider-than-tall shape in the other cases). Reporting color Doppler characteristics was not part of our study, because it is not included as a valid sign in the Kwak-TIRADS score (► **Table 1**).

► **Table 1** Kwak TIRADS score.

TIRADS	definition	features	fitted probability of malignancy
TIRADS 1	normal thyroid parenchyma	–	–
TIRADS 2	benign	–	0 %
TIRADS 3	probably benign	no suspicious feature	2 – 2.8 %
TIRADS 4a	low risk of malignancy	1 suspicious feature	3.6 – 12.7 %
TIRADS 4b	intermediate risk of malignancy	2 suspicious features	6.8 – 37.8 %
TIRADS 4c	moderate risk of malignancy	3 – 4 suspicious features	21 – 91 %
TIRADS 5	high risk of malignancy	5 suspicious features	88.7 – 97.9 %

Suspicious features: 1. solid component, 2. marked hypoechogenicity, 3. microlobulated or irregular margins, 4. micro-calcifications, 5. taller-than-wide shape.

## USE evaluation

USE was performed immediately after US assessment with semi-quantitative Strain Ratio Elastography (SRE) and SWE software for quantitative evaluation (in kPa) and SWE software for quantitative evaluation (in kPa). For USE with SRE evaluation, the operator positioned the transducer perpendicularly in longitudinal scans over the thyroid. A large elastogram region-of-interest (ROI) box was chosen to increase the potential number of samples useful for SRE calculation. Thereafter, the operator applied homogeneous periodic free-hand compression cycles and when the quality-compression bar indicated that the compression was adequate for reliable calculations, 5-second cine-loops were acquired for a preliminary real-time qualitative strain ratio elastography (SRE) evaluation. To obtain a standard evaluation of the ratio between the nodule and the parenchyma, the moment of maximum decompression was selected in a compression cycle, with the most uniform sinusoid de-compression curve and the appropriate amplitude as indicated by the instructions of the software. The hard, suspicious nodules (with lowest elastic strain or no strain) are displayed in blue on the elastogram, the soft nodules (with higher elastic strain) in red and the intermediate values of stiffness with hues of green.

Semiquantitative SRE assessment was carried out by comparing two regions of interest (ROI): ROI 1, including as much nodule area as possible in all frames of the cycle; ROI 2, placed in the adjacent healthy parenchyma, including an area with a similar size and being placed at a similar depth. After placing the ROIs, the US unit immediately calculates the strain ratio value, by dividing the strain of the normal thyroid parenchyma by that of the nodule. The SRE images and values were recorded. Subsequently, for SWE the operator placed the transducer perpendicular to the lesion without pressure, maintaining only slight contact with the skin to minimize compression artifacts [18, 19]. The ROI for measurement was positioned in the lesion. The ultrasound unit uses a Doppler tracking method to calculate shear wave speed. In this technique, push pulse generates downward displacement, parallel to each raster, which can be tracked by color Doppler in order to measure the speed of shear wave propagation.

The US images and the most appropriate USE with SRE and SWE frames and cine-loops were transferred to the local picture archive and communication system (PACS).

## US-guided FNAB, cytology and histology

After US assessment, patients underwent US-guided FNAB of the thyroid nodule with suspicious US or USE features or, in the case of a multinodular thyroid with non-suspicious nodules, the largest thyroid nodule > 15 mm was assessed, excluding anechoic and spongiform nodules (microcysts in > 50 % of volume), according to an internal protocol based on current international guidelines [1, 3, 22]. FNAB was performed in the most suspicious portion of a solid or partially solid nodule, with a 23-gauge needle, free-hand technique and no aspiration. The material was expelled and smeared on glass slides, then placed immediately in 95 % alcohol for Papanicolaou staining. Close collaboration with cyto-pathologists was carried out throughout the study to reduce non-diagnostic specimens.

The cytology interpretation was reported in accordance with the SIAPEC (Italian Society of Anatomical-Pathology) classification (► **Table 2**) approved by the Italian Thyroid Association [23].

Specimens were analyzed by expert thyroid pathologists blinded to US and elastography parameters in all patients that underwent thyroidectomy.

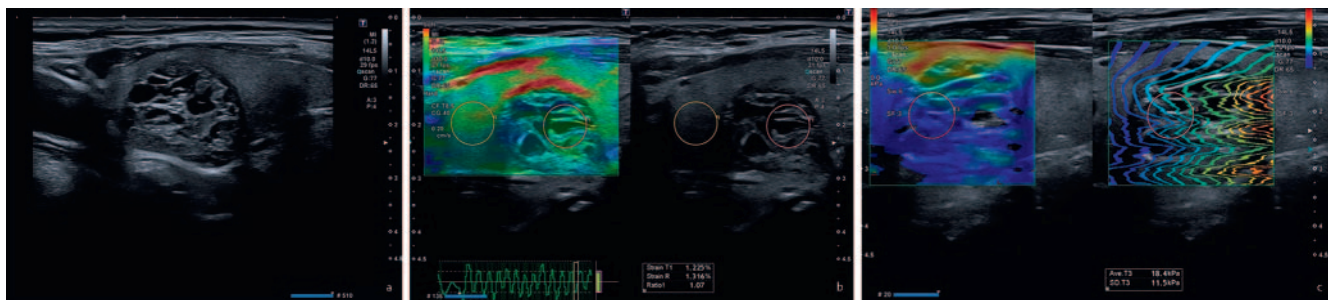
Cytology with a 12-month follow-up US scan showing absence of growth (i. e., increase in diameter of less than 20 % or increase in volume of less than 50 %) or histology performed after surgical treatment was considered the reference standard. Thyroid nodules reported in cytology categories TIR 3b, 4 or 5 or that were growing or causing compressive symptoms underwent surgery (n = 140). In the case of benign cytology, nodules with stable US features were followed up for at least 12 months. When US features were not stable, a second FNAB after 12 months was proposed (n = 103).

## Statistical analysis

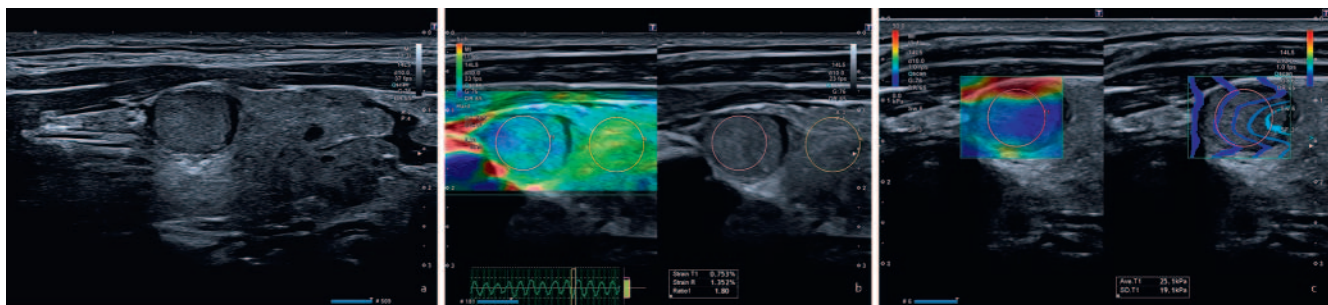
Statistical calculations were performed using Stata software 12.0 (Stata Corporation, College Station, TX, USA). Cut-off values of

► **Table 2** Thyroid cytological classification of the Italian Association of Anatomical Pathology (SIAPEC).

		estimated risk	usual approach
Tir 1	non-diagnostic		
Tir 1c	non-diagnostic because cystic		
Tir 2	non-neoplastic	< 3 %	follow-up
Tir 3A	follicular proliferation of low risk	< 10 %	follow-up
Tir 3B	follicular proliferation of high risk	15 – 30 %	surgery
Tir 4	suspicious for malignancy	60 – 80 %	surgery
Tir 5	malignant	95 %	surgery



► **Fig. 1** a Oval-shaped nodule characterized by mixed content, with some fluid areas on B-mode US (TIRADS 3). b SR evaluation of TIRADS 3 nodule, which appeared soft. c SWE evaluation of TIRADS 3 nodule, which appeared soft.

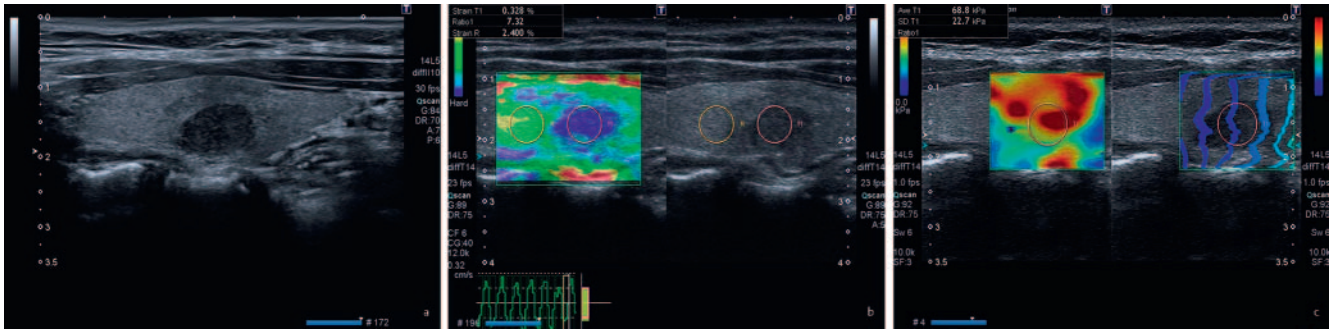


► **Fig. 2** a Oval-shaped, mildly hypoechoic, well-margined nodule on B-mode US (TIRADS 4a); histology showed follicular hyperplasia. b SR evaluation of TIRADS 4a nodule, which appeared soft. c SWE evaluation of TIRADS 4a nodule, which appeared soft

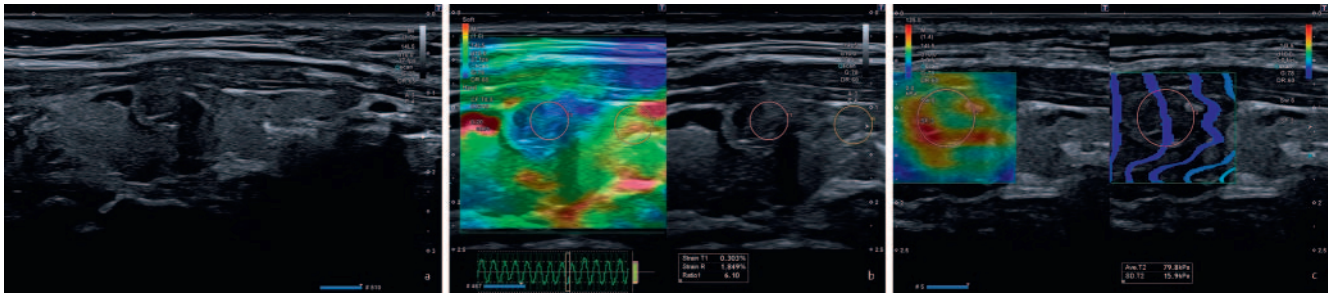
ROC curves were calculated using the Youden test to maximize SRE and SWE sensitivity and specificity and its results were used as the basis for data dichotomization. The analysis of receiver operating characteristic (ROC) curves was used for the assessment of the diagnostic performance of the Kwak-TIRADS score, SE, SRE and SWE. The sensitivity, specificity, positive predictive value (PPV), negative predictive value (NPV) and area under the ROC curve (AUROC) were calculated. The Bonferroni test was used to compare the AUROCs between SRE, TIRADS and SWE. Layering according to nodule size (size < 1 cm, 1 – 2 cm and > 2 cm) was performed. In addition, nodules were also layered according to TIRADS category. A significance threshold was set at  $p = 0.05$ .

## Results

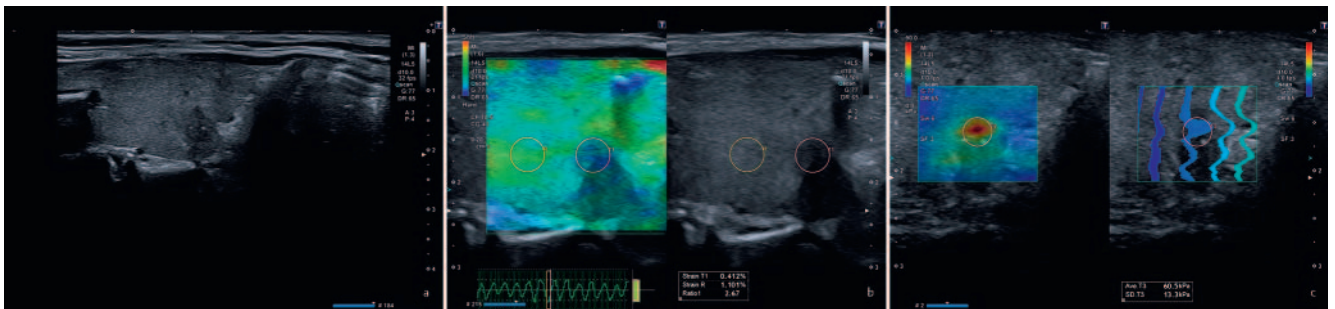
238 patients (70 males; 168 females) with a mean age of 42.3 (18 – 84) years with 271 nodules were examined. 27 patients with 28 nodules were excluded due to: unknown cytology or histology results ( $N = 15$ ), cystic component > 50 % of the nodule ( $N = 5$ ), egg-shell calcifications ( $N = 4$ ), size > 80 % of the lobe ( $N = 4$ ). Finally, 243 nodules in 211 patients (66 males; 145 females) with a mean age of 42.2 (18 – 83) years were included. Of the 243 included nodules, 191 were benign and 52 malignant. Histology of the operated patients ( $N = 140$ ) showed: 86 hyperplastic nodules (► **Fig. 1a – c**, **2a – c**), 3 follicular (► **Fig. 3a – c**), 48 papillary (► **Fig. 4a – c**, **5a – c**), and 1 medullary carcinomas, and 2 follicular adenomas. Patients with histological



► **Fig. 3** a Oval-shaped, hypoechoic nodule on B-mode US (TIRADS 4b). A follicular carcinoma was diagnosed based on histology. **b** SRE evaluation of TIRADS 4b nodule, which appeared stiff. **c** SWE evaluation of TIRADS 4b nodule, which appeared stiff.



► **Fig. 4** a Fairly margined, hypoechoic nodule on B-mode US (TIRADS 4c) with some macrocalcifications. A papillary carcinoma was diagnosed based on histology. **b** SRE evaluation of TIRADS 4c nodule, which appeared stiff. **c** SWE evaluation of TIRADS 4c nodule, which appeared stiff.



► **Fig. 5** a Taller than wide hypoechoic nodule with microcalcifications on B-mode US (TIRADS 5); a papillary carcinoma was diagnosed based on histology. **b** SRE evaluation of TIRADS 5 nodule, which appeared stiff. **c** SWE evaluation of TIRADS 5 nodule, which appeared stiff.

diagnosis of benign nodules underwent surgery either due to symptoms caused by the nodules (48 nodules) or due to Tir3b classification at cytology (40 nodules). The remaining 103 patients had nodules with benign features and follow-up was considered sufficient.

For SRE the optimal cut-off point was 1.92, and for 2D-SWE the optimum cut-off point was 37.5 Kpa.

The Kwak-TIRADS score showed a sensitivity of 59.6%, specificity of 83.8%, PPV of 50.0%, NPV of 88.4% and AUROC of 0.717 in the overall assessment. SRE yielded the best performance with a sensitivity of 82.7%, specificity of 92.7%, PPV of 75.4%, NPV of 95.2% and AUROC of 0.877. SWE showed a sensitivity of 67.3%, specificity of 82.7%, PPV of 51.5%, NPV of 90.3% and AUROC of 0.750 (► **Table 3**, ► **Fig. 6**).

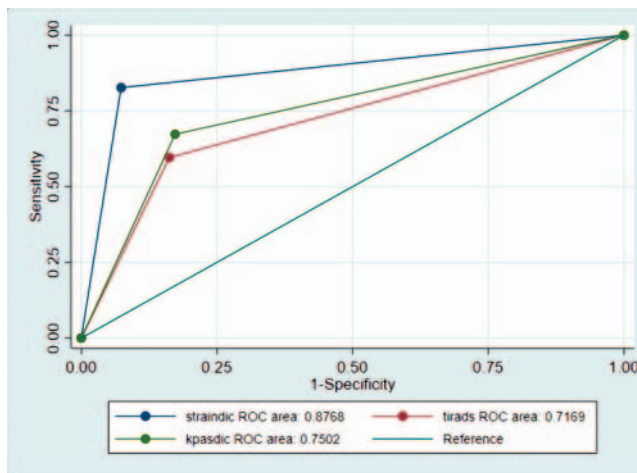
The Bonferroni test (► **Table 4**) showed higher accuracy for SRE with a significantly higher area under the ROC curve for SRE in comparison with Kwak-TIRADS and SWE ( $p < 0.05$ ) as shown in ► **Fig. 6**.

Analysis depending on nodule size resulted in reduced diagnostic sensitivity of TIRADS based on increasing size (sensitivity of 78.9% and specificity of 74.6% for nodules  $< 1$  cm and sensitivity of 44.0% and specificity of 97.5% for nodules  $> 2$  cm) and SWE (sensitivity of 89.5% and specificity of 84.5% for nodules  $< 1$  cm and sensitivity of 55.6% and specificity of 80% for nodules  $> 2$  cm) (► **Table 3**).

The combination of TIRADS with SRE led to a significant increase in the accuracy of the former, although the accuracy of SRE as a standalone method remained higher (► **Table 4**, ► **Fig. 7**). More-

► **Table 3** Performance of TIRADS, SRE and SWE layered according to nodule size.

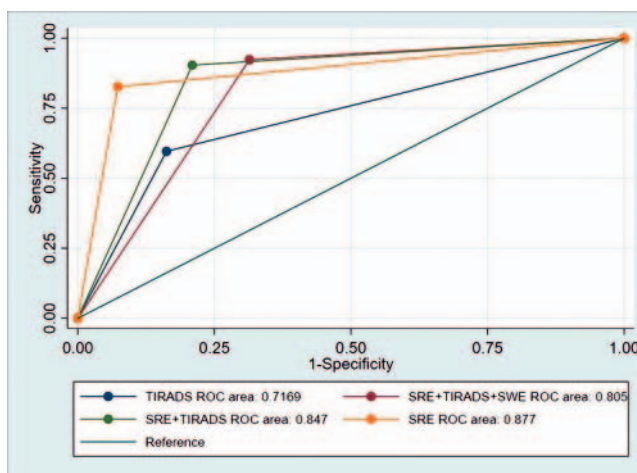
nodules (n)	TIRADS					SRE					SWE					
	Sens (95% CI)	Spec (95% CI)	PPV (95% CI)	NPV (95% CI)	Sens (95% CI)	Spec (95% CI)	PPV (95% CI)	NPV (95% CI)	Sens (95% CI)	Spec (95% CI)	PPV (95% CI)	NPV (95% CI)	Sens (95% CI)	Spec (95% CI)	PPV (95% CI)	NPV (95% CI)
< 1 cm (90)	78.9% (54.4–93.9)	74.6% (62.9–84.2)	45.5% (28.1–63.6)	93% (83–98.1)	78.9% (54.4–93.9)	90.1% (80.7–95.9)	68.2% (45.1–86.1)	94.1% (85.6–98.4)	89.5% (66.9–98.7)	84.5% (74.0–92.0)	60.7% (40.6–78.5)	96.8% (88.8–99.6)	89.5% (66.9–98.7)	84.5% (74.0–92.0)	60.7% (40.6–78.5)	96.8% (88.8–99.6)
1–2 cm (101)	52.2% (30.6–73.2)	85.7% (75.9–92.6)	52.2% (30.6–73.2)	85.7% (75.9–92.6)	87.0% (66.4–97.2)	92.2% (83.8–97.1)	76.9% (56.4–91.0)	95.9% (88.6–99.2)	56.5% (34.5–76.8)	81.8% (71.4–89.7)	48.1% (28.7–68.1)	86.3% (76.2–93.2)	56.5% (34.5–76.8)	81.8% (71.4–89.7)	48.1% (28.7–68.1)	86.3% (76.2–93.2)
> 2 cm (52)	44.4% (13.7–78.8)	97.5% (86.8–99.9)	80% (28.4–99.5)	88.6% (75.4–96.2)	77.8% (40.0–97.2)	100% (91.2–100)	100% (59.0–100)	95.2% (83.8–99.4)	55.6% (21.2–86.3)	80.0% (64.4–90.9)	38.5% (13.9–68.4)	88.9% (73.9–96.9)	55.6% (21.2–86.3)	80.0% (64.4–90.9)	38.5% (13.9–68.4)	88.9% (73.9–96.9)
overall (243)	59.6% (45.1–73.0)	83.8% (77.8–88.7)	50.0% (37.0–63.0)	88.4% (82.8–92.7)	82.7% (69.7–91.8)	92.7% (88.0–95.9)	75.4% (62.2–85.9)	95.2% (91.0–97.8)	67.3% (52.9–79.7)	82.7% (76.6–87.8)	51.5% (39.0–63.8)	90.3% (84.9–94.2)	67.3% (52.9–79.7)	82.7% (76.6–87.8)	51.5% (39.0–63.8)	90.3% (84.9–94.2)



► **Fig. 6** ROC curves according to the cut-off. Strain ratio contains the greatest area under the ROC curve, with a statistically significant difference with TIRADS.

► **Table 4** Comparison of the combination of methods against the TIRADS method alone (standard) by AUROC and Bonferroni test.

	AUROC area	Bonferroni test Pr > chi2
TIRADS	0.7169	0.0006
strain ratio (SRE)	0.8768	0.0006
TIRADS + SRE	0.8472	0.0003
SWE kPa	0.7502	0.0084
TIRADS + SRE + SWE kPa	0.8019	0.0493



► **Fig. 7** The combination of SR with TIRADS (SRE + TIRADS ROC) and SR with TIRADS and SWE kPa (SRE + TIRADS + SWE ROC in graph), both showed an area under the ROC curve greater than TIRADS alone (TIRADS ROC in graph), however smaller than SR alone with statistically significant differences (SRE ROC in graph).

► **Table 5** Diagnostic accuracy of SRE by TIRADS categories.

	malignant nodules	benign nodules	sensitivity (95 % CI)	specificity (95 % CI)	PPV (95 % CI)	NPV (95 % CI)	AUROC (95 % CI)
<b>TIRADS 3</b>							
positive	3	5	50 % (11.8 – 88.2)	95.8% (90.5 – 98.6)	37.5 % (8.52 – 75.5)	97.4% (92.7 – 99.5)	0.73 (0.51 – 0.95)
negative	3	114					
<b>TIRADS 4a</b>							
positive	13	4	86.7 % (59.5 – 98.3)	90.2% (76.9 – 97.3)	76.5 % (50.1 – 93.2)	94.9% (82.7 – 99.4)	0.89 (0.78 – 0.99)
negative	2	37					
<b>TIRADS 4b</b>							
positive	20	2	90.9 % (70.8 – 98.9)	92.6% (75.7 – 99.1)	90.9 % (70.8 – 98.9)	92.6% (75.7 – 99.1)	0.92 (0.84 – 0.99)
negative	2	25					
<b>TIRADS 4c</b>							
positive	3	1	100 % (2.5 – 100)	0 % (0 – 70.8)	25.0 % (0.63 – 80.6)	–	0.5 (0 – 100)
negative	0	0					
<b>TIRADS 5</b>							
positive	6	2	85.7 % (42.1 – 99.6)	50 % (6.8 – 93.2)	75.0 % (34.9 – 96.8)	66.7 % (9.4 – 99.2)	0.68 (0.36 – 0.99)
negative	1	2					

► **Table 6** Diagnostic accuracy of SWE by TIRADS categories.

	malignant nodules	benign nodules	sensitivity (95 % C.I)	specificity (95 % C.I)	PPV (95 % C.I)	NPV (95 % C.I)	AUC (95 % C.I)
<b>TIRADS 3</b>							
positive	0	20	0 % (0 – 45.9 %)	83.2% (75.2 – 89.4 %)	0 % (0 – 16.8 %)	94.3 % (88.0 – 97.9 %)	0.42 (0.38 – 0.45)
negative	6	99					
<b>TIRADS 4a</b>							
positive	10	5	66.7 % (38.4 – 88.2 %)	87.8% (73.8 – 95.9 %)	66.7 % (38.4 – 88.2 %)	87.8 % (73.8 – 95.9 %)	0.77 (0.64 – 0.91)
negative	5	36					
<b>TIRADS 4b</b>							
positive	14	5	63.6 % (40.7 – 82.8 %)	81.5% (61.9 – 93.7 %)	73.7 % (48.8 – 90.0 %)	73.3 % (54.1 – 87.7 %)	0.73 (0.60 – 0.85)
negative	8	22					
<b>TIRADS 4c</b>							
positive	2	1	66.7 % (9.4 – 99.2 %)	0 % (0 – 97.5 %)	66.7 % (9.43 – 9.2 %)	0 % (0 – 97.5 %)	0.33 (0 – 100 %)
negative	1	0					
<b>TIRADS 5</b>							
positive	5	1	71.4 % (29.0 – 96.3)	75.0% (19.4 – 99.4 %)	83.3 % (35.9 – 99.6 %)	60 % (14.7 – 94.7 %)	0.73 (0.43 – 1.0)
negative	2	3					

over, the addition of SWE and SRE to TIRADS did not allow an increase in the AUROC compared to SRE alone.

In addition, performance according to TIRADS categories is also reported (► **Table 5, 6**), showing the clustering of false-positive and false-negative results in TIRADS categories for both SRE and SWE.

## Discussion

Accurate diagnosis of thyroid nodules is a main focus in clinical practice. Conventional ultrasound can detect nodules accurately but has limitations in the differentiation of malignant from benign nodules. Therefore, FNA remains a final minimally invasive diag-

nostic method. However, FNA suffers from limitations related to size, cell sampling as well as e. g. distinction between follicular adenoma vs. carcinoma, suggesting the need for less invasive methods [24]. The ability of different elastography methods (strain elastography and shear wave elastography) to increase the accuracy of ultrasound in the evaluation of thyroid nodules has been extensively discussed in the recent literature, although the evidence remains controversial.

Friedrich-Rust M et al. [25] in a prospective multicenter study showed that SRE as an additional ultrasound tool improves the value of ultrasound for the workup of thyroid nodules and might reduce diagnostic surgery of thyroid nodules.

A meta-analysis in 2015 collected SRE and SWE data from 54 studies (involving 2621 malignant and 7380 benign nodules) and showed that SRE had a better diagnostic sensitivity performance than SWE with comparable specificity between methods. The pooled sensitivity and specificity of SE were 83.0% and 81.2%, respectively, which were higher than SWE – sensitivity: 78.7%, specificity: 80.5%, respectively [26]. In the same year, Liu et al. [27] assessed the pooled diagnostic performance of quantitative shear wave velocity (SWV) measurement on acoustic radiation force impulse (ARFI) elastography in 13 studies with a total of 1854 nodules. The authors suggest that SWE can be used in combination with conventional ultrasound in clinical practice. Another meta-analysis for general ARFI techniques [28] of 16 studies with a total of 2436 nodules found similarly high sensitivity of 0.80 (95% confidence interval [CI], 0.73–0.87) and high specificity of 0.85 (95% CI, 0.80–0.90). Even more recently (2017), Hu et al. [29] published a meta-analysis including 22 articles in which SRE and SWE were compared with respect to differentiating thyroid nodules. Although SRE showed better sensitivity (0.84 vs. 0.79), their specificities were comparable (0.90 vs. 0.87) with an AUROC of 0.94 for SRE and 0.83 for SWE.

Regarding cut-off values, the literature still shows variable data. While the results of Bhatia et al. did not suggest a definitive role for SWE in clinical practice [30], they reported the most accurate SWE cut-off value of 34.5 kPa for a small 2-mm region of interest, yielding a sensitivity of 76.9% and specificity of 71.1% in the diagnosis of papillary carcinoma. EFSUMB and WFUMB guidelines based on literature review suggest US elastography as an additional tool for thyroid lesion differentiation and follow-up of lesions negative for malignancy at FNA with some cut-off values defined [19, 20]. A cut-off value of 22.30 kPa may help to differentiate malignant from benign follicular thyroid lesions (sensitivity 82%, specificity 88%, PPV 75% and NPV 91%). For strain ratio elastography, Cantisani et al. reported a cut-off value of  $\geq 2.0$  to be more likely malignant [31]. This is supported by Zhang et al. [32], who provided the best cut-off value for mean SR  $\geq 2.37$  in predicting malignancy.

Our study is the first in which Kwak-TIRADS, USE with SRE evaluation and 2D-SWE expressed in kPa have been assessed in a relatively large population, with an emphasis on lesion size and results based on a combination of elastography methods. Kwak-TIRADS scoring in our study yielded an overall sensitivity of 59.6%, an overall specificity of 83.8% with an AUROC of 0.717. The Kwak-TIRADS score had its highest sensitivity in the group of nodules  $\leq 1$  cm, 78.9%, and the sensitivity progressively decreased with

an increase in nodule size: 52.2% for nodules between 1–2 cm and 44.4% for nodules greater than 2 cm. However, its specificity increased from 74.6% in nodules  $< 1$  cm to 85.7% in nodules between 1–2 cm, and 97.5% in nodules  $> 2$  cm. SWE (kPa) had a sensitivity and specificity of 67.3% and 82.7%, respectively, with an AUROC of 0.750, a PPV of 51.5% and an NPV of 90.3%. Therefore, it achieved better sensitivity but not specificity than TIRADS but also considering the sensitivity increase it was not statistically significant.

In addition, as well as TIRADS, for 2D-SWE the sensitivity diminishes with increasing nodule size.

SRE yielded the highest performance with an overall sensitivity of 82.7%, specificity of 92.7% with an AUROC of 0.877, significantly higher than Kwak-TIRADS and SWE (► **Table 3, 4**). The sensitivity was 78.9% for nodules  $< 1$  cm; 87% for nodules 1–2 cm; and 77.8% for nodules  $> 2$  cm. In nodules with a size of 1–2 cm, SRE shows higher accuracy, whereas under 1 cm and above 2 cm the difference in accuracy was not significant. This might be due to the fact that smaller and greater nodules are more difficult to target and more heterogeneous in structure, respectively.

Another debated issue is whether the combined use of US and USE may provide better results for thyroid nodule characterization. The accuracy reported by Zhang et al. [32] of the combined use of conventional sonography and ARFI virtual touch tissue imaging (VTI) grade, mean SWE velocity and mean SRE strain ratio was 98.03, 95.39 and 96.71%, respectively, suggestive of high accuracy of all methods. Conversely, Yoon et al. [33] concluded that baseline ultrasound was superior to all additional imaging modalities such as elastography and Doppler US with respect to differentiating thyroid nodules. In the present paper we combined SRE with TIRADS and the 3 techniques altogether. The combined accuracy of TIRADS and SRE was higher than TIRADS alone or SWE and TIRADS (► **Table 5, 6**), but not greater than SRE alone, according to the AUROC ( $p > 0.05$ ). The combined accuracy of the three methods remains lower (the greatest AUROC is for SRE alone, followed by SRE + TIRADS and by SRE + TIRADS + SWE; ► **Fig. 7**). However, the combination of methods as shown in our study resulted in higher sensitivities (SRE and TIRADS combination: 90.4% vs. TIRADS or SRE alone: 59.6% and 82.7%, respectively) but with a lower specificity than SRE alone.

The main limitation of our study is that our institution represents a referral center with a high prevalence of cancer in our cohort. Another limitation of our study is the lack of intra-observer and inter-observer agreement evaluation, because all measurements were performed by only one expert operator.

In conclusion, semiquantitative elastography and quantitative elastography are promising diagnostic tools for discriminating malignant thyroid nodules since both techniques showed higher sensitivity than TIRADS. In particular, SRE also shows significantly higher specificity than TIRADS evaluation by Kwak and higher sensitivity and specificity than SWE. Therefore, considering the limited SWE results shown in the present study and that the combination of TIRADS and SRE achieved better sensitivity, we suggest that SRE should be part of the workup of thyroid nodules, especially to identify malignant lesions sometimes appearing as benign ones on US. However, it should be taken in account that the techniques are operator-, experience-, equipment- and pa-

tient-dependent as already reported [19, 20] and that standardization of the cut-off values is still an active research field.

## Conflict of Interest

Cantisani received honoraria for lectures from Bracco, Samsung and Canon.  
Dietrich CFD received honoraria: Hitachi, Siemens, Supersonic, Mindray, GE, Bracco.  
Radzina received honoraria for lectures from Canon and Bracco.

## References

- [1] Haugen BR, Alexander EK, Bible KC et al. 2015 American Thyroid Association Management Guidelines for Adult Patients with Thyroid Nodules and Differentiated Thyroid Cancer: The American Thyroid Association Guidelines Task Force on Thyroid Nodules and Differentiated Thyroid Cancer. *Thyroid* 2016; 26: 1–133
- [2] Gharib H, Papini E, Garber JR et al. American Association of Clinical Endocrinologists, American College of Endocrinology, and Associazione Medici Endocrinologi medical guidelines for clinical practice for the diagnosis and management of thyroid nodules – 2016 update. *Endocr Pract* 2016; 22: 622–639
- [3] Shin JH, Baek JH, Chung J et al. Ultrasonography Diagnosis and Imaging-Based Management of Thyroid Nodules: Revised Korean Society of Thyroid Radiology Consensus Statement and Recommendations. *Korean J Radiol* 2016; 17: 370–395
- [4] Russ G, Bonnema SJ, Erdogan MF et al. European Thyroid Association Guidelines for Ultrasound Malignancy Risk Stratification of Thyroid Nodules in Adults: The EU-TIRADS. *Eur Thyroid J* 2017; 6: 225–237
- [5] Tessler FN, Middleton WD, Grant EG et al. ACR Thyroid Imaging, Reporting and Data System (TI-RADS): White Paper of the ACR TI-RADS Committee. *J Am Coll Radiol* 2017; 14: 587–595
- [6] Kwak JY, Han KH, Yoon JH et al. Thyroid imaging reporting and data system for US features of nodules: a step in establishing better stratification of cancer risk. *Radiology* 2011; 260: 892–899
- [7] Dietrich CF, Muller T, Bojunga J et al. Statement and Recommendations on Interventional Ultrasound as a Thyroid Diagnostic and Treatment Procedure. *Ultrasound Med Biol* 2018; 44: 14–36
- [8] Tee YY, Lowe AJ, Brand CA et al. Fine-needle aspiration may miss a third of all malignancy in palpable thyroid nodules: a comprehensive literature review. *Ann Surg* 2007; 246: 714–720
- [9] Oertel YC, Miyahara-Felipe L, Mendoza MG et al. Value of repeated fine needle aspirations of the thyroid: an analysis of over ten thousand FNAs. *Thyroid* 2007; 17: 1061–1066
- [10] Grani G, Calvanese A, Carbotta G et al. Intrinsic factors affecting adequacy of thyroid nodule fine-needle aspiration cytology. *Clinical Endocrinology* 2013; 78: 141–144
- [11] Grani G, Lamartina L, Ascoli V et al. Ultrasonography scoring systems can rule out malignancy in cytologically indeterminate thyroid nodules. *Endocrine* 2017; 57: 256–261
- [12] He YP, Xu HX, Zhao CK et al. Cytologically indeterminate thyroid nodules: increased diagnostic performance with combination of US TI-RADS and a new scoring system. *Sci Rep* 2017; 7: 6906
- [13] Horvath E, Silva CF, Majlis S et al. Prospective validation of the ultrasound based TIRADS (Thyroid Imaging Reporting And Data System) classification: results in surgically resected thyroid nodules. *Eur Radiol* 2017; 27: 2619–2628
- [14] Cantisani V, Lodise P, Di Rocco G et al. Diagnostic accuracy and interobserver agreement of Quasistatic Ultrasound Elastography in the diagnosis of thyroid nodules. *Ultraschall in Med* 2015; 36: 162–167
- [15] Razavi SA, Hadduck TA, Sadigh G et al. Comparative effectiveness of elastographic and B-mode ultrasound criteria for diagnostic discrimination of thyroid nodules: a meta-analysis. *Am J Roentgenol* 2013; 200: 1317–1326
- [16] Ghajarzadeh M, Sodagari F, Shakiba M. Diagnostic accuracy of sonoe-elastography in detecting malignant thyroid nodules: a systematic review and meta-analysis. *Am J Roentgenol* 2014; 202: W379–W389
- [17] Nell S, Kist JW, Debray TP et al. Qualitative elastography can replace thyroid nodule fine-needle aspiration in patients with soft thyroid nodules. A systematic review and meta-analysis. *Eur J Radiol* 2015; 84: 652–661
- [18] Cantisani V, Grazhdani H, Ricci P et al. Q-elastosonography of solid thyroid nodules: assessment of diagnostic efficacy and interobserver variability in a large patient cohort. *Eur Radiol* 2014; 24: 143–150
- [19] Cosgrove D, Barr R, Bojunga J et al. WFUMB Guidelines and Recommendations on the Clinical Use of Ultrasound Elastography: Part 4. Thyroid Ultrasound Med Biol 2017; 43: 4–26
- [20] Bamber J, Cosgrove D, Dietrich CF et al. EFSUMB guidelines and recommendations on the clinical use of ultrasound elastography. Part 1: Basic principles and technology. *Ultraschall in Med* 2013; 34: 169–184
- [21] Zhou BG, Wang D, Ren WW et al. Value of shear wave arrival time contour display in shear wave elastography for breast masses diagnosis. *Sci Rep* 2017; 7: 7036
- [22] Milas Z, Shin J, Milas M. New guidelines for the management of thyroid nodules and differentiated thyroid cancer. *Minerva Endocrinol* 2011; 36: 53–70
- [23] Nardi F, Basolo F, Crescenzi A et al. Italian consensus for the classification and reporting of thyroid cytology. *J Endocrinol Invest* 2014; 37: 593–599
- [24] Dighe M, Barr R, Bojunga J et al. Thyroid Ultrasound: State of the Art. Part 2 – Focal Thyroid Lesions. *Med Ultrason* 2017; 19: 195–210. doi:10.11152/mu-999
- [25] Friedrich-Rust M, Vorlaender C, Dietrich CF et al. Evaluation of Strain Elastography for Differentiation of Thyroid Nodules: Results of a Prospective DEGUM Multicenter Study. *Ultraschall in Med* 2016; 37: 262–270
- [26] Tian W, Hao S, Gao B et al. Comparison of Diagnostic Accuracy of Real-Time Elastography and Shear Wave Elastography in Differentiation Malignant From Benign Thyroid Nodules. *Medicine (Baltimore)* 2015; 94: e2312
- [27] Liu BJ, Lu F, Xu HX et al. The diagnosis value of acoustic radiation force impulse (ARFI) elastography for thyroid malignancy without highly suspicious features on conventional ultrasound. *Int J Clin Exp Med* 2015; 8: 15362–15372
- [28] Zhan J, Jin JM, Diao XH et al. Acoustic radiation force impulse imaging (ARFI) for differentiation of benign and malignant thyroid nodules – A meta-analysis. *Eur J Radiol* 2015; 84: 2181–2186
- [29] Hu X, Liu Y, Qian L. Diagnostic potential of real-time elastography (RTE) and shear wave elastography (SWE) to differentiate benign and malignant thyroid nodules: A systematic review and meta-analysis. *Medicine (Baltimore)* 2017; 96: e8282
- [30] Bhatia KS, Cho CC, Tong CS et al. Shear wave elastography of focal salivary gland lesions: preliminary experience in a routine head and neck US clinic. *Eur Radiol* 2012; 22: 957–965
- [31] Cantisani V, D'Andrea V, Biancari F et al. Prospective evaluation of multiparametric ultrasound and quantitative elastosonography in the differential diagnosis of benign and malignant thyroid nodules: Preliminary experience. *Eur J Radiol* 2012; 81: 2678–2683. doi:10.1016/j.ejrad.2011.11.056
- [32] Zhang F, Zhao X, Han R et al. Comparison of Acoustic Radiation Force Impulse Imaging and Strain Elastography in Differentiating Malignant From Benign Thyroid Nodules. *J Ultrasound Med* 2017; 36: 2533–2543. doi:10.1002/jum.14302. Epub 2017 Jun 24
- [33] Yoon JH, Kim EK, Kwak JY et al. Application of Various Additional Imaging Techniques for Thyroid Ultrasound: Direct Comparison of Combined Various Elastography and Doppler Parameters to Gray-Scale Ultrasound in Differential Diagnosis of Thyroid Nodules. *Ultrasound Med Biol* 2018; 44: 1679–1686 doi:10.1016/j.ultrasmedbio.2018.04.006. Epub 2018 May 22